1 **Multi-sensor cloud and aerosol retrieval simulator and**

2 **remote sensing from model parameters – Part 2: Aerosols**

4 **G. Wind[1,2], A. M. da Silva[1], P.M. Norris[1,3], S. Platnick[1], S. Mattoo[1,2] and R. C.**

5 **Levy[1]**

6 [1]{NASA Goddard Space Flight Center, 8800 Greenbelt Rd. Greenbelt, Maryland, 20771,

7 USA}

8 [2]{SSAI, Inc. 10210 Greenbelt Road, Suite 600, Lanham, Maryland 20706, USA}

9 [3]{Universities Space Research Association, 10211 7178 Columbia Gateway Drive,

10 Columbia, MD 21046, USA}

11 Correspondence to: G.Wind (Gala.Wind@nasa.gov)

Abstract

The Multi-sensor Cloud Retrieval Simulator (MCRS) produces a 'simulated radiance' product from any high resolution general circulation model with interactive aerosol as if a specific sensor such as the Moderate Resolution Imaging Spectroradiometer (MODIS) were viewing a combination of the atmospheric column and land/ocean surface at a specific location. Previously the MCRS code only included contributions from atmosphere and clouds in its radiance calculations and did not incorporate properties of aerosols. In this paper we added a new aerosol properties module to the MCRS code that allows user to insert a mixture of up to 15 different aerosol species in any of 36 vertical layers.

This new MCRS code is now known as MCARS (Multi-sensor Cloud and Aerosol Retrieval Simulator). Inclusion of an aerosol module into MCARS not only allows for extensive, tightly controlled testing of various aspects of satellite operational cloud and aerosol properties retrieval algorithms; but also provides a platform for comparing cloud and aerosol models against satellite measurements. This kind of two-way platform can improve the efficacy of model parameterizations of measured satellite radiances, allowing to assess model skill consistently with the retrieval algorithm. The MCARS code provides dynamic controls for appearance of cloud and aerosol layers. Thereby detailed quantitative studies of the impacts of various atmospheric components can be controlled.

In this paper we illustrate the operation of MCARS by deriving simulated radiances from various data fields output by the Goddard Earth Observing System version 5 (GEOS-5) model. The model aerosol fields are prepared for translation to simulated radiance using the same model subgrid variability parameterizations as are used for cloud and atmospheric properties profiles, namely the Independent Column Approximation (ICA) technique. After MCARS computes modeled sensor radiances equivalent to their observed counterparts, these radiances are presented as input to operational remote sensing algorithms.

1   Specifically, the MCARS computed radiances are input into the processing chain used to

2   produce the MODIS Data Collection 6 aerosol product (M{O/Y}D04). The M{O/Y}D04

3   product is of course normally produced from M{O/Y}D021KM MODIS Level-1B radiance

4   product directly acquired by the MODIS instrument. MCARS matches the format and

5   metadata of a M{O/Y}D021KM product. The resulting MCARS output can be directly

6   provided to MODAPS (MODIS Adaptive Processing System) as input to various operational

7   atmospheric retrieval algorithms. Thus the operational algorithms can be tested directly

8   without needing to make any software changes to accommodate an alternative input source.

9   We show direct application of this synthetic product in analysis of the performance of the

10   MOD04 operational algorithm. We use biomass burning case studies over Amazonia

11   employed in a recent Working Group on Numerical Experimentation (WGNE) -sponsored

12   study of aerosol impacts on Numerical Weather Prediction (Freitas et al. 2016). We

13   demonstrate that a known low bias in retrieved MODIS aerosol optical depth appears to be

14   due to a disconnect between actual column relative humidity and the value assumed by the

15   MODIS aerosol product.

1 Introduction

Aerosols in the atmospheric column are a significant source of uncertainty for passive remote-sensing (e.g. from a satellite) retrievals of cloud optical and microphysical properties. Thick aerosol layers can be wrongly identified as clouds, and aerosols above clouds will lead to biases in cloud retrievals (Meyer et al. 2013). Biases in cloud detection and retrievals of cloud microphysics will lead to uncertainties in properties important for quantifying Earth's radiative budget. On the other hand, clouds wrongly identified and retrieved as aerosol may have similar impacts on estimates of aerosol radiative forcing and effects on climate and clouds. The Moderate-resolution Imaging Spectroradiometer (MODIS; Barnes et al. 1998) has been flying on the polar orbiting (at 705 km altitude) satellites known as Terra (since 2000) and Aqua (since 2002). Viewing a 2300 km swath, split into 5-minute granules, MODIS measures radiance (or reflectance) in 36 spectral channels, of which 19 are in reflective solar bands, with the other 17 being terrestrial infrared emission. All bands are in at least 1 km spatial resolution. Based on MODIS observations, separate teams have created high-quality retrievals of both cloud (e.g. the M{O/Y}D06_L2 (MxD06); Platnick et al, 2003) and aerosol (M{O/Y}D04_L2 (MxD04; Levy et al., 2013) properties. Current operational cloud retrieval includes methods for clearing the aerosols mis-identified as clouds from retrieval attempts. (Zhang and Platnick 2011; Pincus et al. 2012). Similarly for aerosol retrievals, much effort is made to reclassify as "not cloudy" scenes that are in fact, heavy dust or smoke. Therefore, for both teams, uncertainty whether a particular sample is cloud-covered or contains primarily aerosols, and how to propagate this uncertainty into retrieval products, remains a topic of great interest. A major problem is that there is no absolute ground-truth to confirm or deny these decisions in all cases. Ground based instrumentation such as sun photometers (Holben et al 1998) may not be able to accurately distinguish between aerosol and thin clouds due to limited spectral range, generally reaching only up to a wavelength of 1.024μm. Newer sun

1   photometers do provide information up to 1.64μm, but they are not present at every ground

2   site. The ground sites in Brazil that fall within the area we studied in this paper carry the older

3   instrumentation. The best wavelengths for detecting cirrus clouds are located around 1.38 and

4   1.8 μm. There are also efforts to retrieve aerosol optical depth above cloud layers (Meyer and

5   Platnick 2015, Meyer et al. 2013). Validation for such algorithms is often done using lidar and

6   radar data (Ackerman, et al. 2008, Notarnicola, et al. 2011). However as current spaceborne

7   lidar and radar instruments have fixed nadir view, the amount of such data acquired in tandem

8   with an instrument like MODIS is rather limited.

9   While a global meteorological model cannot be directly used to validate observations and

10   retrievals due to the many assumptions and simplifications commonly made in the dynamic

11   core and physics parameterizations (Rienecker et al. 2008), one can use such a model to learn

12   about sensitivities of retrieval algorithms. As global models such as the Goddard Earth

13   Observing System Model, Version 5 (GEOS-5; Rienecker et al. 2008, Molod et al. 2012),

14   become increasingly realistic when simulating aerosols and clouds over complex surface

15   terrain, we can apply detailed radiative transfer (RT) to simulate how these scenes would

16   appear to a satellite such as MODIS, and how operational algorithms would in turn retrieve

17   the specified conditions. Since the specified model aerosol and cloud properties of the scene

18   are known, one can then characterize the ability (and uncertainties) of standard (e.g. MxD04

19   or MxD06) retrievals in these scenes. Thus, one can evaluate the current (and possibly

20   historical) performance of cloud and aerosol properties retrievals. Application and evaluation

21   of these simulation capabilities for known instruments is also an important step in

22   development of Observing System Simulation Experiments for future observing missions.

23   The Multi-Sensor Cloud and Aerosol Retrieval Simulator (MCARS; Wind et al., 2013) is

24   a modular, flexible tool, in which model output is coupled with a radiative transfer code in

1   order to simulate Top Of Atmosphere (TOA) radiances that may be measured by a remote

2   sensing instrument if it were passing over the model fields. In principle, MCARS can be

3   applied to any model / visible-IR radiometer combination. The simulation complexity is only

4   limited by computer power. However, in this paper, the MCARS continues to use the

5   combination of GEOS-5 model and Discrete Ordinate Radiative Transfer (DISORT) code

6   (Stamnes et al. 1988) to simulate MODIS radiances. In Wind et al. (2013), the MCARS

7   simulated only clouds; here we add microphysical properties of aerosols present in scenes we

8   examine.

9   The approach we take is to populate the operational MODIS Level 1B calibrated radiance

10   files with TOA radiances simulated from GEOS-5 model output and DISORT. For a given

11   time and location, MODIS provides a particular geometry of observation. Since GEOS-5

12   simulates clouds and aerosols interactively, we can replace the MODIS-observed reflectance

13   data with the simulated radiance product derived from the model. Then we run the standard

14   aerosol (MxD04_L2) and cloud (MxD06_L2) retrieval codes and compare retrieval result to

15   the known GEOS-5 source data. The discrepancies diagnosed by this device can then be

16   contrasted to discrepancies obtained by comparing the real operational retrievals to

17   independent, trusted observations (e.g., AOD from AErosol RObotic NETwork

18   (AERONET)). To the extent that simulated and real statistical comparisons match, we can use

19   capabilities of the MCARS code to examine the causes for such discrepancies, and hopefully

20   identify opportunities for algorithm improvement. Since the aerosol retrieval is under-

21   determined (Levy et al. 2013) and a number of assumptions must be made, the MCARS

22   simulation approach is highly valuable as individual assumptions can be tested in isolation.

23   The MCARS code has sufficient flexibility to test impacts of settings of single operational

24   retrieval code parameters without interference from other components.

1   Section 2 describes the GEOS-5 aerosol properties and their addition into MCARS.

2   Section 3 describes the MODIS aerosol product. Section 4 discusses case selection for the

3   current analysis. It shows the selected scenes simulated by MCARS and describes other

4   special simulation settings available that provide additional analysis capabilities. This section

5   also presents analysis of retrieved aerosol properties as compared to the specified "ground"

6   truth that served as input to the simulations. Finally, section 5 discusses next steps in the

7   continuing MCARS development.

9   **2   GEOS-5 aerosol model and data assimilation systems**

10   **2.1   System Description**

11   Global aerosol, cloud, surface and atmospheric column fields from the GEOS-5 model

12   and data assimilation system serve as the starting point for radiance simulations. The GEOS-5

13   system contains components for atmospheric circulation and composition (including aerosol

14   and meteorological data assimilation), ocean circulation and biogeochemistry, and land

15   surface processes. Components and individual parameterizations within components are

16   coupled under the Earth System Modeling Framework (ESMF, Hill et al. 2004). This study is

17   based on the near real-time (NRT) configuration of GEOS-5 where sea surface temperature

18   and sea ice are specified from observations (Molod et al. 2012). The Goddard Chemistry

19   Aerosol Radiation and Transport (GOCART, Colarco et al. 2010, Chin et al. 2002) bulk

20   aerosol scheme is used in the GEOS-5 NRT aerosol forecasting system in this paper. A

21   version of GOCART is run online and affects atmospheric radiative heating and budget in

22   GEOS-5. GOCART treats the sources and sinks of dust, sulfate, sea salt and black

23   and organic carbon aerosols. Total mass of sulfate, and hydrophobic and hydrophilic modes

24   of carbonaceous aerosols are tracked. Dust and sea salt have an explicit particle size

1   distribution with five non-interacting size bins for each constituent. Emission functions of

2   both dust and sea salt depend on wind speed. Sulfate and carbonaceous species have

3   contributions primarily from fossil fuel combustion, biomass burning, and biofuel

4   consumption, with additional biogenic sources of organic carbon. Sulfate has additional

5   chemical production from oxidation of SO_2 and dimethyl sulfide (DMS). We additionally

6   include a database of volcanic SO_2 emissions and injection heights (Diehl et al. 2012). For all

7   aerosol species, optical properties are obtained primarily from the commonly used Optical

8   Properties of Aerosols and Clouds (OPAC) data set (Hess et al. 1998). We have recently

9   updated our dust optical properties data set to incorporate non-spherical dust properties based

10 on the work of Meng et al. (2010), Colarco et al. (2013) and Buchard et al. (2014). The

11 aerosol transport is consistent with the underlying atmospheric dynamics and physical

12 parameterizations (e.g., moist convection and turbulent mixing) of the model.

13   The GEOS-5 meteorological data assimilation is based on the Grid-point Statistical

14 Interpolation (GSI) analysis scheme, jointly developed with National Oceanic and

15 Atmospheric Administration National Center for Environmental Prediction (NOAA/NCEP)

16 (Wu et al. 2002; Kleist et al. 2009). While the current GEOS-5 operational algorithm is based

17 on a hybrid ensemble-variational scheme, the results reported here are based on the original

18 3D-Var implementation (Rienecker et al 2008). The aerosol re-analysis is produced at three-

19 hour intervals, with assimilation of bias-corrected aerosol optical depth from MODIS, and has

20 been evaluated against ground-base sun photometer measurements (Holben et al., 1998)

21 and against the Multi-angle Imaging Spectroradiometer (MISR) satellite instrument (Kahn et

22 al, 2007).

2.2 Fire Emissions

The fire emissions used in our simulations come from the Quick Fire Emission Dataset (QFED) Version 2.4 (Darmenov and da Silva, 2015). The QFED emissions are based on a top-down approach relating satellite retrieved Fire Radiative Power (FRP) at the top of the atmosphere to the amount of gases and particulate matter being emitted at the burning surface. The QFED emission factors are tuned so as to promote agreement among modeled and observed AOD. Another unique feature of QFED is how it handles areas obstructed by clouds when estimating grid-box mean emission rates. A sequential, minimum-variance algorithm keeps track of the fractional obscured area of given grid box. Emissions under the obscured area are then obtained by means of damped persistency model. Details can be found in Darmenov and da Silva (2015).

2.3 Case study selection

The WMO's Working Group on Numerical Experimentation (WGNE) has organized an exercise to evaluate the impact of aerosols on Numerical Weather Prediction (NWP) (Freitas et al. 2015.) This exercise involves testing of regional and global models currently used for weather forecasting by operational centers worldwide. The authors of this exercise selected 3 strong or persistent events of aerosol pollution worldwide that could be fairly represented by current NWP models. These cases were specifically selected to facilitate evaluation of the aerosol impact on weather prediction. We chose one of the specified WGNE events: an extreme case of biomass burning smoke in Brazil, as the focus of this paper.

3 MODIS aerosol product

The MODIS "dark-target" (DT) aerosol product is described in detail in Levy, et al. (2013) and references therein. In this section we will give a brief overview of the DT algorithm as applied to MODIS observations.

The standard MODIS aerosol properties retrieval algorithm is a 10 km resolution product calculated from a detailed analysis of 10x10 boxes of 1km MODIS pixels. A necessary constraint for the algorithm is that the underlying surface is dark in visible and shortwave-IR wavelengths. There are two separate algorithm paths for ocean and land.

Pixels that are suspected to be cloudy or too bright or too noisy are discarded using conditions described in (Levy et al, 2007). Once the data sample is prepared, a spectral profile of average TOA spectral reflectance is created and compared against a lookup table. If a match is found, values for aerosol optical depth (AOD) and fine-mode aerosol weighting (FMW) are then returned.

In this paper we will focus on the land algorithm. Full description of the ocean algorithm can be found in Levy, et al (2013). Over land, even though there is greater variability of underlying surface than over ocean and thus greater uncertainty in retrieved aerosol properties, aerosol retrieval is still achievable. Over vegetated and dark-soiled surfaces, Kaufman et al. (1997) found that surface reflectance values for red (e.g. 0.65 μm) and blue (0.47 μm) wavelengths are correlated with the surface reflectance in a short-wave infrared (SWIR) band (e.g. 2.13 μm). The land algorithm uses 0.47, 0.65 and 2.13μm channels for the main retrieval and 0.55, 0.86 and 1.24μm channels to give additional surface constraints.

The aerosol LUT is calculated for black surfaces and sea-level pressure. There are three fine particle model types and one coarse particle model type of aerosols used for dust based on climatology of AERONET inversion data (Dubovik et al, 2002). Each model type is multi-lognormal and is represented by size distribution, particle shape and complex refractive indices. The three fine-dominated models are differentiated primarily by single scattering albedo (SSA) in mid-visible wavelengths: urban/industrial type (SSA~0.95), near-source biomass burning (SSA~0.85) and a moderately absorbing type (SSA~0.90) to cover all other cases. For each aerosol type, the LUT includes TOA reflectance for a variety of angles and

1   AOD referenced to 0.55µm.

2   Even with the constraints on surface reflectance, the aerosol retrieval does not have

3   enough information to select between different aerosol types. Therefore, the relative

4   proportion of fine-mode and coarse-mode aerosols must be prescribed so that, coupled with

5   surface constraints, a best match can be found in the LUT for TOA spectral reflectance in the

6   blue, red and SWIR wavelengths. The difference between TOA and nearest LUT reflectance

7   is the fitting error.

8   With Levy et al., (2013) and previous studies, the primary validation of the MODIS

9   product is by detailed co-location with ground-based sun photometer data, especially the

10   Aerosol Robotic Network (AERONET; Holben et al., 1998). In this way, Levy et al., (2013)

11   have defined the expected error (EE) envelope for the 0.55 µm AOD as $\pm(0.05 + 15\%;)$.

12   While spectral surface reflectance is also retrieved, it does not tend to compare well with

13   values obtained from the sun photometers. Note that the EE is defined upon mutually

14   retrieved data. This means that satellite and sun photometer both observe enough clear-sky to

15   retrieve AOD.

16   Also, while AERONET is well distributed about the globe, there are many situations for

17   which MODIS retrieves aerosol, but there are no AERONET data available to compare with.

18   Thus, there is no way to determine whether the MODIS aerosol retrieval has made reasonable

19   choices, either for pixel selection, for cloud screening, or for aerosol model type and surface

20   reflectance assumptions.

21   This motivates our use of the MCARS. Having full knowledge of underlying

22   atmospheric, cloud, aerosol and surface parameters MCARS allows us to see deeper than

23   AERONET would and over a much wider spatial area.

4   MCARS simulations

4.1   The MCARS software

We produced the simulation input data in accordance with the methods outlined in Wind et al. (2013). The GEOS-5 model output is split into 1-km subcolumns using the ICA method as described in detail in Wind et al. (2013). Here we give a brief summary of the model data preparation methodology.

Sampling of model cloud-related fields to the MODIS pixel scale is not straightforward because cloud properties typically vary on scales not adequately resolved by the operational 0.25° GEOS-5 resolution. To sample cloud fields, 1 km MODIS pixels for each GEOS-5 gridcolumn are collected and the same number of pixel-like sub-columns are generated using a statistical model of sub-gridcolumn moisture variability. The general approach of Norris et al. (2008) is followed, namely using a parameterized probability density function (PDF) of total water content for each model layer and a Gaussian copula to correlate these PDFs in the vertical. Full details of the calculation of this PDF are described fully in Norris and da Silva (2016).

The subcolumns generated in this way are horizontally independent, but are subsequently "clumped," or rearranged, to give horizontal spatial coherence, by using a horizontal Gaussian copula applied to condensed water path. This clumping acts to give the generated clouds a reasonable horizontal structure, such that the cloudy pixels in a gridcolumn are actually grouped into reasonable looking clouds, rather than being randomly distributed. This is important because the MODIS cloud optical and microphysical properties retrieval algorithm has some spatial variance tests for potentially partially-cloudy pixels, removing cloud edges by the so-called "clear-sky restoral" (Zhang and Platnick 2011; Pincus et al. 2012). If clumping is not used, then individual points generated by ICA stand an exceptionally high

1   chance of being eliminated by the clear sky restoral unless a model grid box has a nearly

2   100% cloud fraction.

3   The layer aerosol properties are obtained using the independent column approximation

4   with the same PDF of total water content as used for clouds. The MCARS code uses a species

5   file, produced from the GEOS-5 model output, which for each simulated MODIS pixel gives

6   individual aerosol optical depths by aerosol type. The OPAC database (Hess et al, 1998) is

7   then queried in order to obtain the aerosol phase function for each of the 15 aerosol species

8   and the properties such as single-scattering albedo are then augmented by profile of

9   subcolumn relative humidity. The result of this query is a set of Legendre coefficients and a

10   single-scattering albedo that correspond to the combined effect of all 15 aerosol species.

11   Model parameters such as profiles of temperature, pressure, ozone and water vapor

12   together with layer information about clouds (and now aerosols) are combined with solar and

13   view geometry of the MODIS instrument. Surface information is also a combination of

14   GEOS-5 information of surface temperature, snow and sea ice cover and MODIS-derived

15   spectral surface albedo (Moody et al. 2007, 2008). All these parameters are transferred to the

16   DISORT-5 radiative transfer code and reflectances and radiances in 24 MODIS channels are

17   produced. They are output into a standard MODIS L1B file that corresponds to the source

18   MODIS geolocation file we used to sample the model output with. All metadata is preserved

19   in this process and so the MCARS output is indistinguishable from a real MODIS granule

20   except in how it may appear to the user's eye. These synthetic reflectances and radiances are

21   completely transparent to any operational or research-level retrieval algorithm code and can

22   be used for any purpose that real sensor data can.

23   In order to produce these simulations we use the NASA Center for Climate Simulations

24   (NCCS) supercomputer Discover. It takes 5.5 hours of wall clock time on 144 processors to

25   produce one complete simulation. The performance can be improved if the user limits the

simulation scope to fit a particular investigation they are working on. For example, an aerosol

researcher would not likely need to simulate the MODIS channels that they would not use and

thus reduce execution time by at least half. Because these simulations are simultaneously used

for both cloud and aerosol work, we simulate all the channels that would be used by both

cloud and aerosol disciplines.

4.2 Granule selection

In order to perform tests of the MCARS aerosol module we have selected Aqua MODIS

granules from time period corresponding to WGNE selection for biomass burning in Brazil.

In this paper we specifically present results from simulations based on two granules of smoke

in Brazil 2012 day 252 17:30 UTC and day 254 17:20 UTC subsequently referred as "Brazil

1" and "Brazil 2".

5 Analysis

For each granule, we ran the simulations in several modes with varied run-time option

settings. For example, the cloud-only mode corresponds to a clean atmosphere with no

aerosols; this mode was the only one considered in Wind et al. (2013). In the current paper we

consider additional options afforded by the implementation of the aerosol effect. The cloud-

free option runs atmosphere and aerosols without any clouds. When clouds are turned off, we

do not alter the humidity profiles to dry the atmosphere out; because of the high relative

humidity conditions where clouds are present, aerosol hygroscopic effects are pronounced

there as well. The full simulation option includes atmosphere (temperature, humidity and

ozone profiles), all clouds and all aerosols. There is also an additional option where the user

can remove both clouds and aerosols and be left with just the atmosphere itself. Rayleigh

scattering is always included by default but user also has control over whether or not to turn it

off. While this no-cloud/no-aerosol mode could be useful for studies of atmospheric

1 correction methods, we do not exercise it here, as our primary goal here is to investigate the

2 performance of the MODIS aerosol algorithms.

3   The cloud-free mode of operation is convenient when complex cloud and aerosol scenes

4 are being investigated and one wishes to quantify or remove possible impacts of cloud

5 contamination on the retrieval. Figure 1 shows RGB images constructed from simulated

6 MODIS L1B for the different modes of execution for the "Brazil 1" case. MODIS aerosol

7 retrievals were produced for radiance simulations including atmosphere, cloud and aerosols

8 (Figure 1c) and for radiance simulations excluding clouds (Figure 1d). Rayleigh scattering is

9 included in these simulations.

10   These Brazil cases came from source MODIS Aqua granules and had been processed

11 using the MODIS Aqua aerosol properties retrieval algorithm. Therefore in this section we

12 will use MYD04 designation for the MODIS aerosol properties retrieval result. There are

13 some slight differences between the MODIS Terra (MOD04) and MODIS Aqua (MYD04)

14 algorithms due to calibration differences between the two instruments (Levy et al, 2013).

15   The scatter diagrams in Figure 2 compare AOD retrieved using the MYD04 algorithm to

16 the specified GEOS-5 AOD, which is considered the ground truth in this case. MODIS

17 aerosol retrievals are commonly compared to co-located AERONET AOD measurements

18 (Correia and Pires 2006, Levy, et al. 2007, Remer et al. 2005) for validation. Unlike

19 comparisons of actual MODIS data with AERONET, the match ups in Figure 2 did not

20 require any temporal averaging or aggregation because for every MYD04 retrieval there is a

21 directly corresponding input data point with all aerosol, cloud and atmospheric properties

22 readily available. The overall shape of resulting scatter plots turned out to be quite similar to

23 existing MYD04 – AERONET comparisons for this region such as those that appear in

24 Correia and Pires (2006) and Figure 3. Figure 3 shows an actual comparison for AERONET

25 observations for months of July and August and all available Aqua MODIS collocated

1   observations from year 2002 through 2015. The chosen AERONET sites:

2   Campo_Grande_SONDA, Sao_Paulo and CUIABA-MIRANDA fall in the general area of the

3   two Brazil cases selected for study. They of course represent a tiny sample of the

4   geographical area covered by the MCARS data, just three points out of 2.7 million collocated

5   samples that MCARS provides, but they display a similar shape of the relationship between

6   ground truth and MYD04 retrieval.

7   MCARS is a fully configurable system where source input for all synthetic radiances can

8   be controlled at all times, so that any resulting retrieval can be examined in great detail

9   insofar as the particular setup of model input and radiative transfer core allows. For these

10   smoke cases we used these capabilities to investigate further the specific reasons why the

11   MYD04 retrievals tend to underestimate AOD for smoke aerosol.

12   The first test we made was to examine the performance of MYD04 cloud mask, which is

13   an aerosol specific product (Remer et al, 2005), different from the operational MODIS cloud

14   mask product (Ackerman et al, 2006). The main purpose of this analysis was to ascertain

15   whether cloud contamination could account for some of the discrepancies. Individual panels

16   in Figure 2 show the results of retrievals run with and without the cloud layers. Panels a) and

17   b) show result for "Brazil 1" and panels c) and d) are for "Brazil 2". "Brazil 1" case does not

18   show any significant cloud contamination. The MYD04 cloud mask does a very good job of

19   avoiding cloud. "Brazil 2" does show some very minor cloud contamination as evident by a

20   small cluster of high MYD04 AOD and low GEOS-5 AOD that disappears when clouds are

21   removed from simulation. However the overall shape of the scatter plot when clouds are

22   removed remains unchanged.

23   The aerosol models used in the MYD04 retrievals make assumptions about the smoke

24   aerosol optical properties, which may not match the aerosol optical assumptions in GEOS-5

25   (Levy et al, 2007). In cases of complex aerosol mixtures or if the model selected by the

1 MYD04 algorithm does not correspond to the aerosols provided by GEOS-5, large retrieval

2 errors should result. Figure 4 shows the species mixture for "Brazil 1" (a) and "Brazil 2" (b)

3 cases. They are both dominated by carbon, organic carbon from smoke in particular, with

4 very little, if any contribution from other species. Therefore these particular cases can be

5 treated as having a single aerosol type present without significant error. MYD04 retrieval

6 output indicates that either moderately or strongly absorbing smoke had been selected, which

7 is very appropriate for the selected granules. Thus any discrepancy in selection of aerosol

8 model does not explain the scatter plot shape.

9 Another candidate source of retrieval error is any difference between the phase functions

10 assumed by MYD04 and GEOS-5. We ran the initial simulations simply using the Henyey-

11 Greenstein (HG) phase function approximation and then repeated the same simulation using

12 the phase functions provided by the OPAC database described in section 2. Figure 5 shows

13 the result for "Brazil 1" and "Brazil 2" cases using the cloud-free run with HG phase function

14 versus OPAC phase function. For the smoke aerosol cases studied, the specific phase

15 function shape does not appear to have a significant impact on the differences seen between

16 MYD04 and GEOS-5.

17 An additional potential source of error for aerosol retrievals over land is the surface

18 albedo and its variation over a 10x10 km area. We performed a simulation where we selected

19 a single surface albedo profile from a successful MYD04 retrieval and fixed the surface

20 albedo to that particular surface albedo profile for the entire granule. The test albedo profile

21 used is listed in Table 1. The profile corresponds to a very dark vegetated surface, the ideal

22 conditions for the MYD04 land algorithm. Figure 6 shows the effect of using a constant

23 surface albedo for "Brazil 1" and "Brazil 2" cases. Whereas use of constant surface albedo

24 reduces the scatterplot spread and so allows us to potentially quantify the effect of surface

25 inhomogeneity on MYD04 land retrievals, it does not alter the overall bias characteristics of

1   scatter plots.

2   With all the factors of model selection, surface parameters and cloud contamination taken

3   into account, we now turn our attention to the aerosol scattering properties, the spectral single

4   scattering albedo (SSA) in particular. Figures 7 and 8 show the spectral profile of aerosol SSA

5   for "Brazil 1" and "Brazil 2" cases respectively for the first seven MODIS channels. This

6   aerosol SSA is a bulk quantity, integrated over all layers and combines all 15 available

7   aerosol species. However the cases under consideration are heavily dominated by carbon with

8   negligible amounts of dust and sulfate. In this particular case the additional uncertainties that

9   would arise from a mixture of aerosols with different scattering properties do not present an

10   issue. The single scattering albedo remains quite high until we reach the 1.2µm channel,

11   MODIS band 5, and beyond. Then it drops precipitously. AERONET is only able to provide

12   direct inversion retrievals of single scattering albedo for four wavelengths out to a maximum

13   wavelength of 1.024 µm (Dubovik and King, 2000; Dubovik et al., 2002).. The rapid change

14   in single scattering albedo for smoke aerosol modeled in GEOS-5 is related to aerosol

15   humidification effects, both dilution effects and hygroscopic growth (Colarco et al. 2010,

16   2013). The net effect is that when humidity decreases, so does the single scattering albedo.

17   Figure 9 shows a plot of OPAC single scattering albedo for a variety of column relative

18   humidity values as a function of wavelength. (Colarco, et al 2013) The operational MODIS

19   aerosol code assumes a constant 80% relative humidity when the lookup tables are generated

20   (Levy et al, 2007). It is a reasonable assumption as long as one does not attempt to use

21   channels with wavelengths that are longer than 0.8µm. The MYD04 algorithm however does

22   use the 2.1µm MODIS channel in retrieval, a channel that is sensitive to humidity. MCARS is

23   particularly well suited to test for humidity impact on the retrieval accuracy. We made another

24   experiment with fixed surface albedo, OPAC aerosol phase function shape but we used the

25   constant single scattering albedo values from the MODIS aerosol algorithm in the reflectance

1   calculation that serves as input to the retrieval algorithm. The result is shown in figure 10.

2   When humidification effects are not taken in consideration in the SSA calculation, MYD04

3   retrieval results closely line up with synthetic GEOS-5 source data. The underestimate of

4   aerosol optical depth disappears, with "Brazil 2" showing the most dramatic improvement. It

5   appears that if MYD04 were to take into account humidification effects and implement a

6   correction for single scattering albedo value as a function of column relative humidity, the

7   result of comparison between MODIS and AERONET could be significantly improved for

8   biomass burning cases in Brazil and other locations with similar synoptic conditions.

9   The improvement is limited however to AOD higher than about 0.5. Relative humidity

10   does not appear to have an effect on retrieved low AOD values. MYD04 product does not

11   provide pixel-level retrieval uncertainty estimates. It is possible that the inherent uncertainty

12   in performing retrieval using such small signal is so high that it drowns out other effects.

13   More studies may be conducted as to attempt to create a pixel-level estimate of retrieval

14   uncertainty for aerosol optical properties retrievals.

15   The MODIS aerosol product performs a simultaneous retrieval of land surface

16   reflectance and aerosol optical depth. After looking at the behavior of aerosol optical depth

17   and making a recommendation for a possible improvement in the retrieval algorithm, we

18   examined the retrieval of land surface reflectance. The MODIS aerosol product provides

19   retrieved land surface reflectance in the 0.47, 0.65 and 2.1μm channels. We looked at the land

20   surface reflectance for the simulation of figure 10 panels c) and d) that now matched the

21   source aerosol optical depth reasonably well. The simulation was run under constant surface

22   albedo conditions and we would have expected to see a result, with some degree of

23   uncertainty of course, that would match the given constant surface albedo. However the

24   retrieved land surface reflectance appeared to be a near-linear function of aerosol optical

25   depth. One possible explanation for this behavior may involve the assumed fraction of coarse-

1   mode aerosol in the aerosol model mixture. To examine this hypothesis we performed a

2   MYD04 retrieval using an aerosol model setting so that MYD04 retrieval only used fine mode

3   particles. The retrieval results, depicted in figure 11 confirm that the near co-linearity of

4   surface reflectance and AOD was indeed directly related to fraction of coarse mode particles,

5   such as dust, in the assumed aerosol mixture. Of course there is no way to know exactly what

6   fraction of coarse mode particles may be present in the mixture as the MODIS DT algorithm

7   does not have enough information content to constraint the fine/coarse mode fraction over

8   land (Levy et al, 2007). However, it can be noted that if such co-linearity is seen during a

9   specific local aerosol study maybe during a field campaign, it may be suggested that the

10   coarse mode fraction assumed operationally for that particular region may be too high. An

11   analysis of MODIS operational retrievals to identify locations and times where this co-

12   linearity exists may be useful to identify regions where the assumed coarse/fine mode fraction

13   might need to be adjusted. Figure 11 illustrates the impact of coarse-mode fraction selection

14   on land surface reflectance retrievals for "Brazil 1" and "Brazil 2" cases. The fine-to-coarse

15   mode ratio does not appear to have an impact on the low bias of MYD04 AOD retrieval vs.

16   "ground truth" comparisons presented in the earlier figures.

17   **6   Conclusions and future directions**

18   This paper is a continuation of work started in Wind et al, (2013). The multi-sensor cloud

19   retrieval simulator code (MCRS) had been extended to add aerosol effects to radiance

20   simulations. The current implementation of the MCARS code generates synthetic radiances

21   by sending GEOS-5 model fields and MODIS sensor geometry and location information to

22   the DISORT-5 radiative transfer core. The radiance and reflectance data are output in a

23   standard MODIS Level 1B format that can be transparently ingested by any retrieval or

24   analysis code that reads data from the MODIS instrument.

25   After the aerosol properties module had been added to the MCARS code we used the

1   simulator to perform detailed analysis of performance of the operational MODIS dark target

2   aerosol properties retrieval product for the Aqua MODIS instrument (MYD04). We found the

3   cause of known low bias in MYD04 retrieved AOD for smoke when compared to in-situ

4   measurements. We suggest that the MYD04 retrieval might consider using column relative

5   humidity from ancillary data when performing retrievals in regions that are defined to be

6   dominated by smoke aerosols. The mismatch between the aerosol single scattering albedo

7   assumed by MYD04 and the given synthetic single scattering albedo is the cause of the low

8   bias at higher AODs. The impact of surface inhomogeneity is also quantifiable. Whereas it

9   may not be possible to make an operationally actionable item from retrieval behavior when

10   surface is made homogeneous, it may be possible to deduce an estimate of retrieval

11   uncertainty due to land surface effects.

12   This study is a good example of capabilities of the MCARS code. We are planning many

13   more studies of retrieval algorithm performance.

14   The MCARS results give a relationship between aerosol single scattering albedo, bias in

15   retrieved aerosol optical depth and column relative humidity. One of our future directions is

16   to examine further this relationship and possibly establish a solid parameterization that could

17   be used by the modeling community to reduce biases in assimilated observations that might

18   display a similar low bias when compared to in-situ measurements.

19   The MCARS simulator is currently being extended to calculate synthetic radiances for

20   the Meteosat Second Generation Spinning Enhanced Visible Infrared Radiometer Imager

21   (MSG-SEVIRI).

22   **7   Code and Data Availability**

23   The MCARS code and any datasets produced, including all data shown (GEOS-5 input

24   in netCDF4 and all MODIS output in HDF4 file format) and discussed in this paper, are

25   available to users free of charge by contacting the authors and becoming a registered user of

1 this software package so that any updates to code or datasets can be issued directly. There

2 may be additional, wider distribution means in the future as needed. We have not deemed it

3 practical up to this time to release the MCARS source code into general-purpose source

4 repositories. The data files are quite large with source input data being on the order of 20 Gb

5 for each MODIS-like granule created. The GEOS-5 model source code is publicly available

6 and we may release the MCARS code under the same NASA Open Source Agreement and

7 the same repository in the coming year.

Acknowledgements

The authors would like to thank Leigh Munchak of the MODIS Aerosol Group for providing Figure 3 and Peter Colarco of the Goddard Modeling and Assimilation Office for providing us with Figure 9. The authors would like to thank Brad Wind for the initial idea for creating a simulator, the output of which could be transparently used with remote sensing retrieval codes. This research was supported by the NASA Radiation Sciences Program. Resources supporting this work were provided by the NASA High-End Computing (HEC) Program through the NASA Center for Climate Simulation (NCCS) at the Goddard Space Flight Center.

1   **References**

2   Ackerman, A., K. Strabala, P. Menzel, R. Frey, C. Moeller, L. Gumley, B. Baum, S. W.

3   Seemann, and H. Zhang, 2006: Discriminating clear-sky from cloud with MODIS

4   Algorithm Theoretical Basis Document (MOD35). ATBD Reference Number: ATBD-

5   MOD-35. http://modis-atmos.gsfc.nasa.gov/reference_atbd.html LAD:07.23.2013

6   Ackerman, S. A., R.E. Holz, R. Frey, E. W. Eloranta, B.C. Maddux, M. McGill, 2008: Cloud

7   Detection with MODIS. Part II: Validation. J. Atm. Ocn. Tech, 25, 1073-1086, doi:

8   10.1175/2007JTECHA1053.1

9   Barnes, W. L., T. S. Pagano, and V. V. Salomonson, 1998: Prelaunch characteristics of the

10   Moderate Resolution Imaging Spectroradiometer (MODIS) on EOS-AM1. IEEE Trans.

11   Geosci. Remote Sens., 36, 088–1100.

12   Buchard, V., A. da Silva, P. R. Colarco, A. Darmenov, C. A. Randles, R. Govindaraju, O.

13   Torres, J. Campbell, and R. Spurr, 2015. Using the OMI aerosol index and absorption

14   aerosol optical depth to evaluate the NASA MERRA aerosol reanalysis. Atmos. Chem.

15   Phys, 15, 5743-5760. doi: 10.5194/acp-15-5743-2015.

16   Buchard, V., A. M. da Silva, P. Colarco, N. Krotkov, R.R. Dickerson, J. W. Stehr, G. Mount,

17   E. Spinei, H. L. Arkinson, and H. He, 2014: Evaluation of GEOS-5 sulfur dioxide

18   simulations during the Frostburg, MD 2010 field campaign, Atmos. Chem. Phys., 14,

19   1929–1941, doi:10.5194/acp-14-1929-2014

20   Chin, M., P. Ginoux, S. Kinne, O. Torres, B. N. Holben, B. N. Duncan, R. V. Martin, J. A.

21   Logan, A. Higurashi, and T. Nakajima, 2002: Tropospheric Aerosol Optical Thickness

22   from the GOCART Model and Comparisons with Satellite and Sun Photometer

23   Measurements. J. Atmos. Sci., 59, 461–483.

1   Colarco, P., A. da Silva, M. Chin, T. Diehl, 2010: Online simulations of global aerosol

2   distributions in the NASA GEOS-4 model and comparisons to satellite and ground-based

3   aerosol optical depth. J. Geophys. Res., 115, D14207, doi:10.1029/2009JD012820

4   Colarco, P. R., E. P. Nowottnick, C. A. Randles, B. Yi, B., P. Yang, K.-M. Kim, J. A. Smith,

5   and C. G. Bardeen, 2013: Impact of Radiatively Interactive Dust Aerosols in the NASA

6   GEOS-5 Climate Model: Sensitivity to Dust Particle Shape and Refractive Index, Journal

7   of Geophysical Research, doi:10.1002/2013JD020046.

8   Correia, A., C. Pires 2006: Validation of aerosol optical depth retrievals by remote sensing

9   over Brazil and South America using MODIS. Anais do XIV Congresso Brasileiro de

10   Meteorologia.

11   Darmenov, Anton, and Arlindo da Silva, 2015. The Quick Fire Emissions Dataset (QFED):

12   Documentation of versions 2.1, 2.2 and 2.4. NASA/TM–2015–104606, Vol. 38.

13   Diehl, T., A. Heil, M. Chin, X. Pan, D. Streets, M. Schultz, and S. Kinne , 2012:

14   Anthropogenic, biomass burning, and volcanic emissions of black carbon, organic carbon,

15   and SO2 from 1980 to 2010 for hindcast model experiments. Atmos. Chem. Phys.,

16   12(9):24895-24954

17   Dubovik, O., B. N. Holben, T. F. Eck, A. Smirnov, Y. J. Kaufman, M. D. King, D. Tanré,

18   I. Slutsker, 2002: Variability of absorption and optical properties of key aerosol types

19   observed in worldwide locations J. Atmos. Sci., 59, 590-608

20   Dubovik, O., M.D. King, 2000: A flexible inversion algorithm for retrieval of aerosol optical

21   properties from sun and sky radiance measurements J. Geophys. Res., Vol. 105, 20673-

22   20696

23   Freitas, S. A. da Silva, A. Benedetti, G. Grell, O. Jorba, M. Mokhtari, 2015: Evaluating

1   Aerosol Impacts on Numerical Weather Prediction: A WGNE Initiative. Symposium on

2   Coupled Chemistry-Meteorology/Climate Modeling, Switzerland 23-25 February 2015

3   Frey, R. A., S. A. Ackerman, Y. Liu, K. I. Strabala, H. Zhang, J. Key and X. Wang, 2008:

4   Cloud Detection with MODIS, Part I: Recent Improvements in the MODIS Cloud Mask,

5   JTECH 25, 1057-1072.

6   Hess, M., P. Koepke, and I. Schult, 1998: Optical properties of aerosols and clouds: The

7   software package OPAC. B. Am. Meteorol. Soc., 79(5), 831–844.

8   Hill, C., C. DeLuca, V. Balaji, M. Suarez, A. da Silva, 2004: The architecture of the Earth

9   System Modeling Framework, Comp. Sci. Engr., 6(1), 18-28.

10   Holben, B. N., T. F. Eck, I. Slutsker, D. Tanre, J. P. Buis, A. Setzer, E. F. Vermote, J. A.

11   Reagan, Y. J. Kaufman, T. Nakajima, F. Lavenu, I. Jankowiak, A. Smirnov, 1998:

12   AERONET – A federated instrument network and data archive for aerosol characterization.

13   Rem. Sens. Env., v.66, n1, p1-16.

14   Kahn, R. A., M. J. Garay, D. L. Nelson, K. K. Yau, M. A. Bull, B. J. Gaitley, J. V.

15   Martonchik, and R. C. Levy, 2007: Satellite-derived aerosol optical depth over dark water

16   from MISR and MODIS: Comparisons with AERONET and implications for

17   climatological studies, J. Geophys. Res., 112, D18205, doi:10.1029/2006JD008175.

18   Kaufman, Y. J., A. E. Wald, L. A. Remer, B. C. Gao, R. R. Li, L. Flynn, 1997: The MODIS

19   2.1μm channel - Correlation with visible reflectance for use in remote sensing of aerosol

20   IEEE Trans. Geosci. Remote Sens., Vol. 35, 1286-1298

21   Kleist, D. T., D. F. Parrish, J. C. Derber, R. Treadon, W-S. Wu, S. Lord, 2009: Introduction of

22   the GSI into the NCEP Global Data Assimilation System. Wthr and Fcst., 1691-1705, DOI:

23   10.1175/2009WAF2222201.1

1   Levy, R. C., S. Mattoo, L. A. Munchak, L. A. Remer, A. M. Sayer, F. Patadia, and N. C.

2   Hsu, 2013: The Collection 6 MODIS aerosol products over land and ocean, Atmos. Meas.

3   Tech., 6, 2989-3034, doi:10.5194/amt-6-2989-2013

4   Levy, R. C., L. A. Remer, S. Mattoo, E. F. Vermote, Y. J. Kaufman, 2007: Second-generation

5   operational algorithm: Retrieval of aerosol properties over land from inversion of Moderate

6   Resolution Imaging Spectroradiometer spectral reflectance. J. Geophys. Res.-Atmos., 112,

7   D13211, doi: 10.1029/2006JD007811.

8   Levy, R.C., L. A. Remer, D. Tanre, S. Mattoo, Y.J. Kaufman, 2009: Algorithm for remote

9   sensing of tropospheric aerosol over dark targets from MODIS Collections 005 and 051,

10   revision 2. ATBD Reference Number: ATBD-MOD-04. http://modis-

11   atmos.gsfc.nasa.gov/reference_atbd.html

12   Meng, Z., P. Yang, G. W. Kattawar, L. Bi, K. N. Liou and I. Laszlo, 2010.: Single-scattering

13   properties of tri-axial ellipsoidal mineral dust aerosols: A database for application to

14   radiative transfer calculations, J. Aerosol Sci., 41, 501–512

15   Meyer, K. G., S. E. Platnick. 2015: Simultaneously inferring above-cloud absorbing aerosol

16   optical thickness and underlying liquid phase cloud optical and microphysical properties

17   using MODIS. *J. Geophys. Res. Atmos*, 120 (11): 5524–5547

18   Meyer, K. G., S. E. Platnick, L. Oreopoulos, and D. Lee. 2013: Estimating the direct radiative

19   effect of absorbing aerosols overlying marine boundary layer clouds in the southeast

20   Atlantic using MODIS and CALIOP. *J. Geophys. Res. Atmos.,* 118 (10): 4801-4815

21   Molod, A., L. Takacs, M. Suarez, J. Bacmeister, I.-S. Song, and A. Eichmann, 2012: The

22   GEOS-5 Atmospheric General Circulation Model: Mean Climate and Development from

23   MERRA to Fortuna. Tech. Rep. S. Gl. Mod. Data Assim., 28

1 Moody, E. G., M. D. King, C. B. Schaaf, D. K. Hall, and S. Platnick, 2007: Northern

2   Hemisphere five-year average (2000-2004) spectral albedos of surfaces in the presence of

3   snow: Statistics computed from Terra MODIS land products. Remote Sens. Environ., 111,

4   337–345.

5 Moody, E. G., M. D. King, C. B. Schaaf and S. Platnick, 2008: MODIS-derived spatially

6   complete surface albedo products: Spatial and temporal pixel distribution and zonal

7   averages. J. Appl. Meteor. Climatol., 47, 2879–2894.

8 Norris, P. M., L. Oreopoulos, A. Y. Hou, W.-K. Tao, X. Zeng, 2008: Representation of 3D

9   heterogeneous cloud fields using copulas: Theory for water clouds. J. Q. R. Meteorol. Soc.

10   134: 1843–1864. doi:10.1002/qj.321.

11 Norris, P. M. and A. M. da Silva, 2016: Monte Carlo Bayesian inference on a statistical model

12   of sub-gridcolumn moisture variability using high-resolution cloud observations. Part I:

13   Method. Accepted to Q. J. R. Meteorol. Soc.

14 Notarnicola, C., D. Di Rosa, F. Posa, 2011: Cross-Comparison of MODIS and CloudSat Data

15   as a Tool to Validate Local Cloud Cover Masks. Atmos., 2, 242-255,

16   doi:10.3390/atmos2030242

17 Pincus, R., S. Platnick, S. A. Ackerman, R. S. Hemler, and R. J. P. Hofmann, 2012:

18   Reconciling simulated and observed views of clouds: MODIS, ISCCP, and the limits of

19   instrument simulators. J. Climate, 25, 4699-4720. doi:10.1175/JCLI-D-11-00267.1.

20 Platnick, S., M. D. King, S. A. Ackerman, W. P. Menzel, B. A. Baum, J. C. Riedi, and R. A.

21   Frey, 2003: The MODIS cloud products: Algorithms and examples from Terra. IEEE

22   Trans. Geosci. Remote Sens., 41, 459–473.

23 Remer, L. A., Y. J. Kaufman, D. Tanre, S. Mattoo, D. A. Chu, J.V. Martins, 2005: The

1 MODIS aerosol algorithm, products, and validation. J. Atm. Sci. 62, 947–973.

2 doi:10.1175/JAS3385.1

3 Rienecker, M.M., M. J. Suarez, R. Todling, J. Bacmeister, L. Takacs, H.-C. Liu, W. Gu, M.

4 Sienkiewicz, R. D. Koster, R. Gelaro, I. Stajner, and J. E. Nielsen, 2008: The GEOS-5 Data

5 Assimilation System - Documentation of Versions 5.0.1, 5.1.0, and 5.2.0. Tech. Rep. S. Gl.

6 Mod. Data Assim., 27

7 Wind, G., da Silva, A. M., Norris, P. M., and Platnick, S.: Multi-sensor cloud retrieval

8 simulator and remote sensing from model parameters – Part 1: Synthetic sensor radiance

9 formulation, Geosci. Model Dev., 6, 2049-2062, doi:10.5194/gmd-6-2049-2013, 2013.

10 Wu, W. S., R. J. Purser, D. F. Parrish, 2002: Three-dimensional variational analysis with

11 spatially inhomogeneous covariances. Mon. Wea. Rev., 130, 2905-2916

12 Zhang, Z., and S. Platnick, 2011: An assessment of differences between cloud effective

13 particle radius for marine water clouds from three MODIS spectral bands. J. Geophys.

14 Res., 116, D20215, doi:10.1029/2011JD016216.

2 Table 1: Constant surface albedo setting used in smoke AOD retrieval investigation

MODIS channel	Central Wavelength (μm)	Surface Albedo
1	0.65	0.027
2	0.86	0.288
3	0.47	0.017
4	0.55	0.037
5	1.24	0.252
6	1.63	0.146
7	2.13	0.054
8	0.41	0.014
9	0.44	0.022
17	0.91	0.283
18	0.94	0.280
19	0.94	0.280
20	3.7	0.038
22	3.9	0.038
26	1.38	0.216
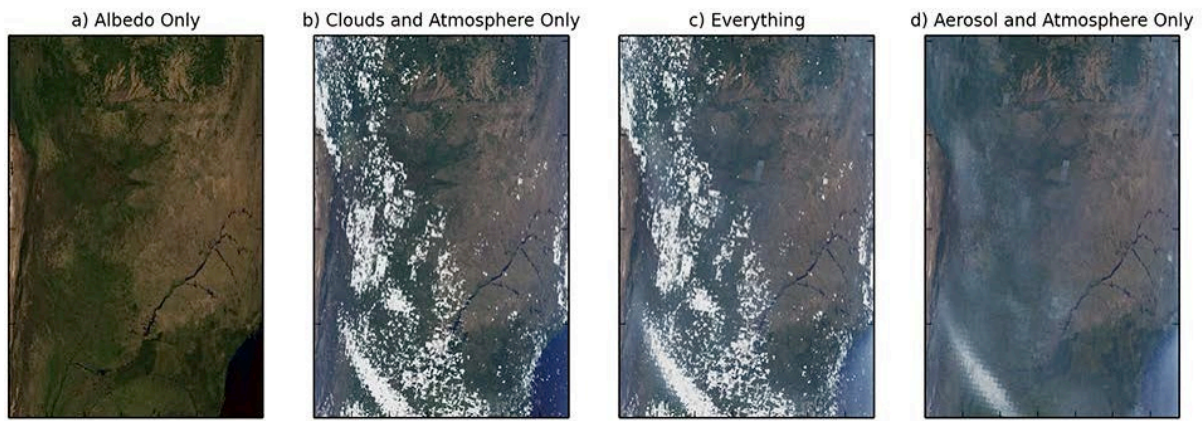
2   Figure 1. Example of various execution modes of the MCARS code using the "Brazil 1" case

3   2012 day 252 17:30UTC. Panel a) shows the atmosphere-free image, just the surface albedo.

4   Panel b) shows the clouds-only simulation with no aerosols. Panel c) has both clouds and

5   aerosols and panel d) shows the cloud-free mode, where cloud layers have been removed

6   from the scene. Panels b), c) and d) all include Rayleigh scattering.
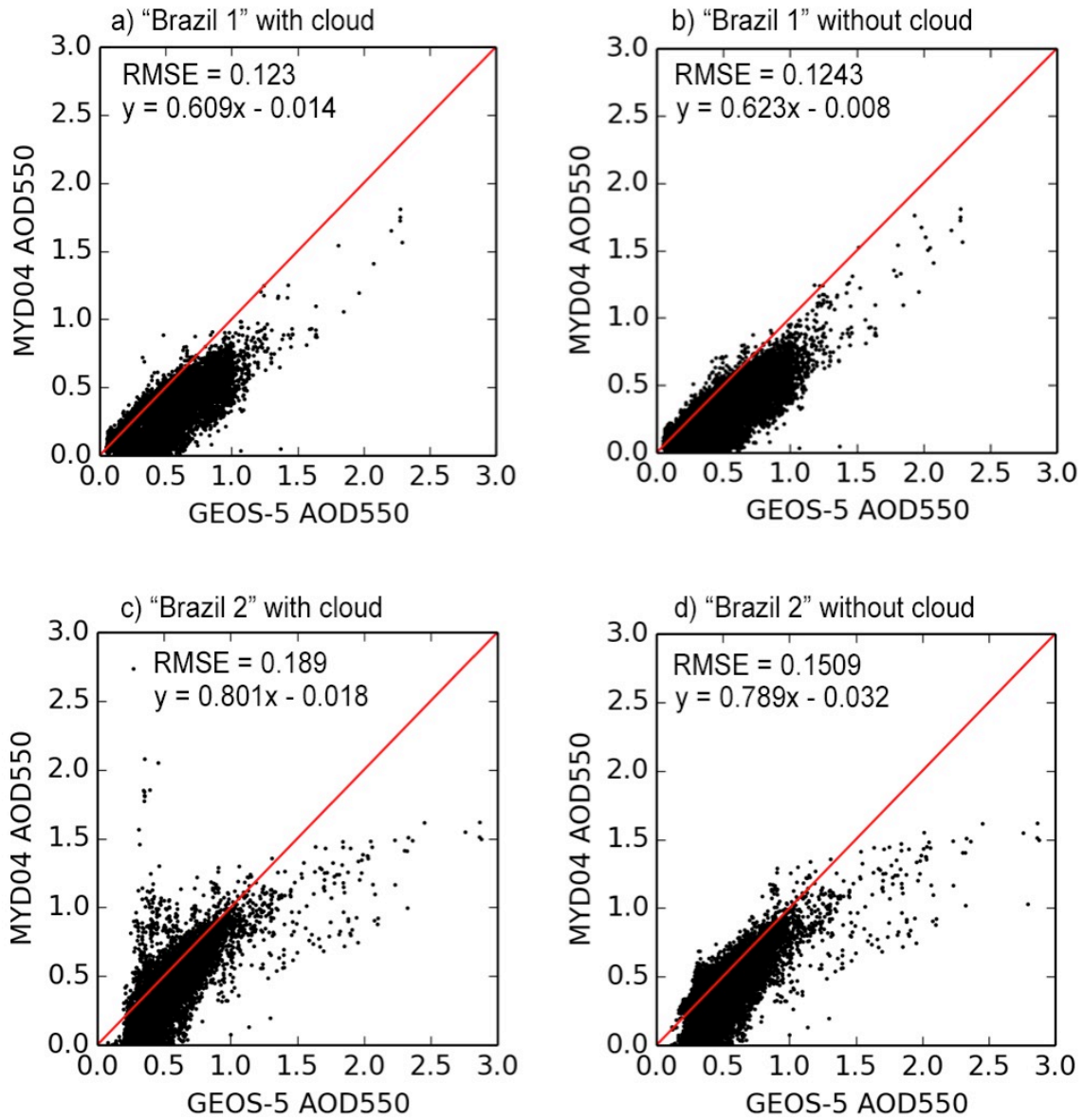
Figure 2. MYD04 retrieval of 550 nm aerosol optical depth vs ground "truth" of GEOS-5 550

nm aerosol optical depth. Panel a) shows the scatterplot for retrieval from simulation in figure

1c and panel b) shows retrieval from simulation in figure 1d for "Brazil 1" case. Panels c) and

d) show same information for "Brazil 2" case.
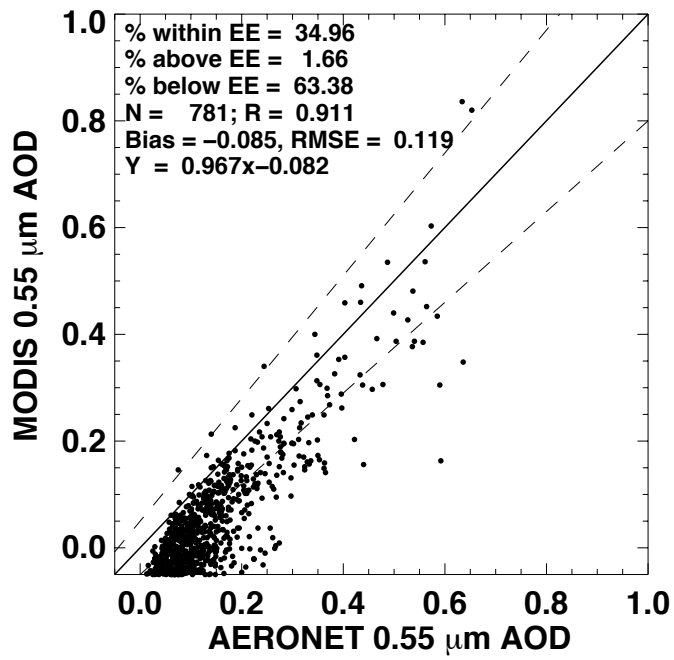
2   Figure 3. Comparison of actual AERONET measurements and operational Aqua MODIS

3   Collection 6 aerosol product for Brazil sites Campo_Grande_SONDA, Sao_Paulo and

4   CUIABA-MIRANDA in the general area of MCARS granules.
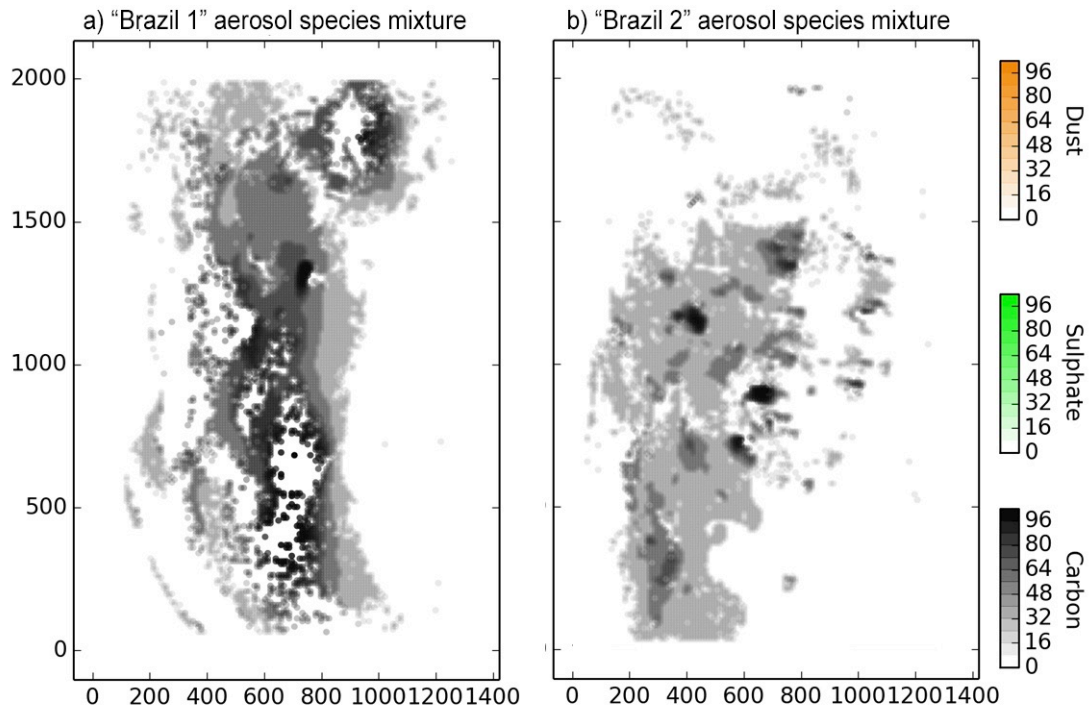
2 Figure 4. GEOS-5 aerosol species mixture for attempted MYD04 retrievals in figure 2. Panel

3 a) shows the "Brazil 1" case (2012 day 252) and panel b) shows the "Brazil 2" case (2012 day

4 254). Both are dominated by carbon (smoke) aerosol.
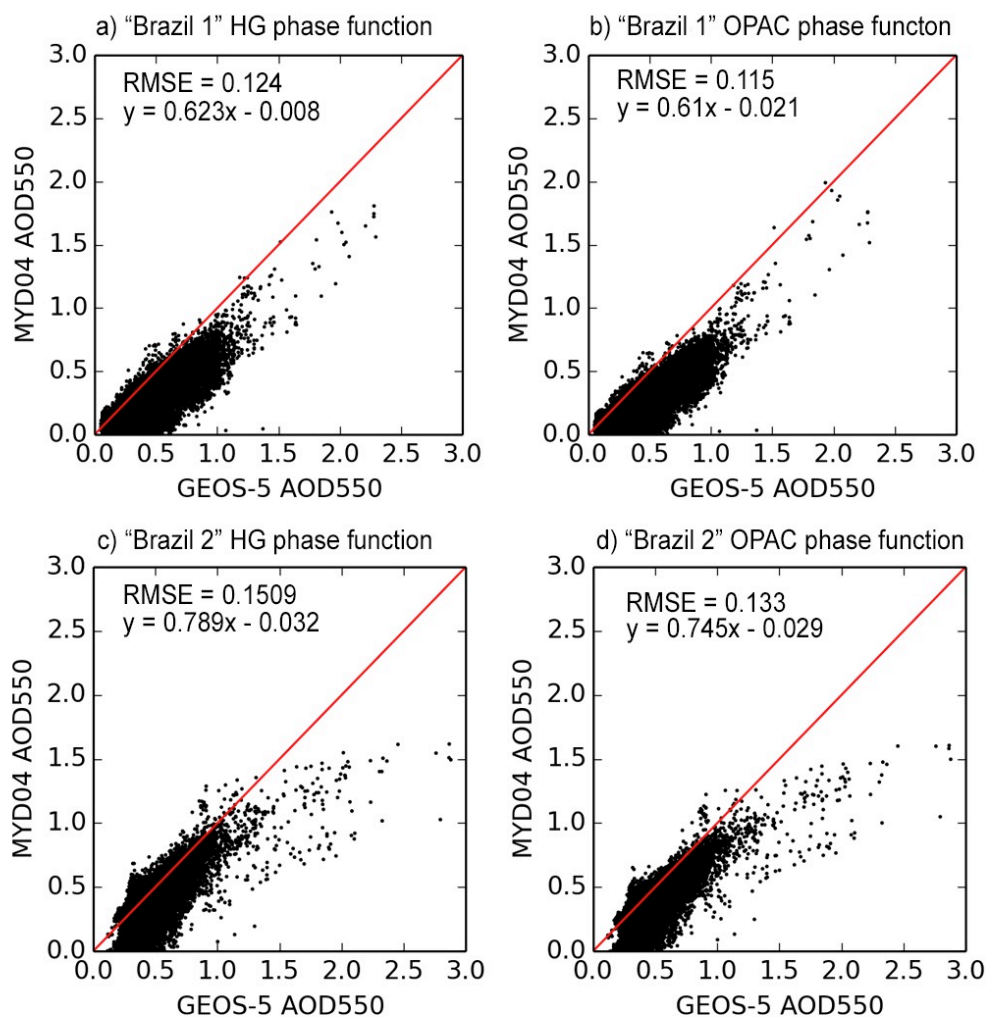
Figure 5. Effect of aerosol phase function shape on Brazil smoke cases. Panels a) and c) show the runs with HG phase function. Panels b) and d) show use of the OPAC composite phase function.

2
3
4
5
6
7
8
9
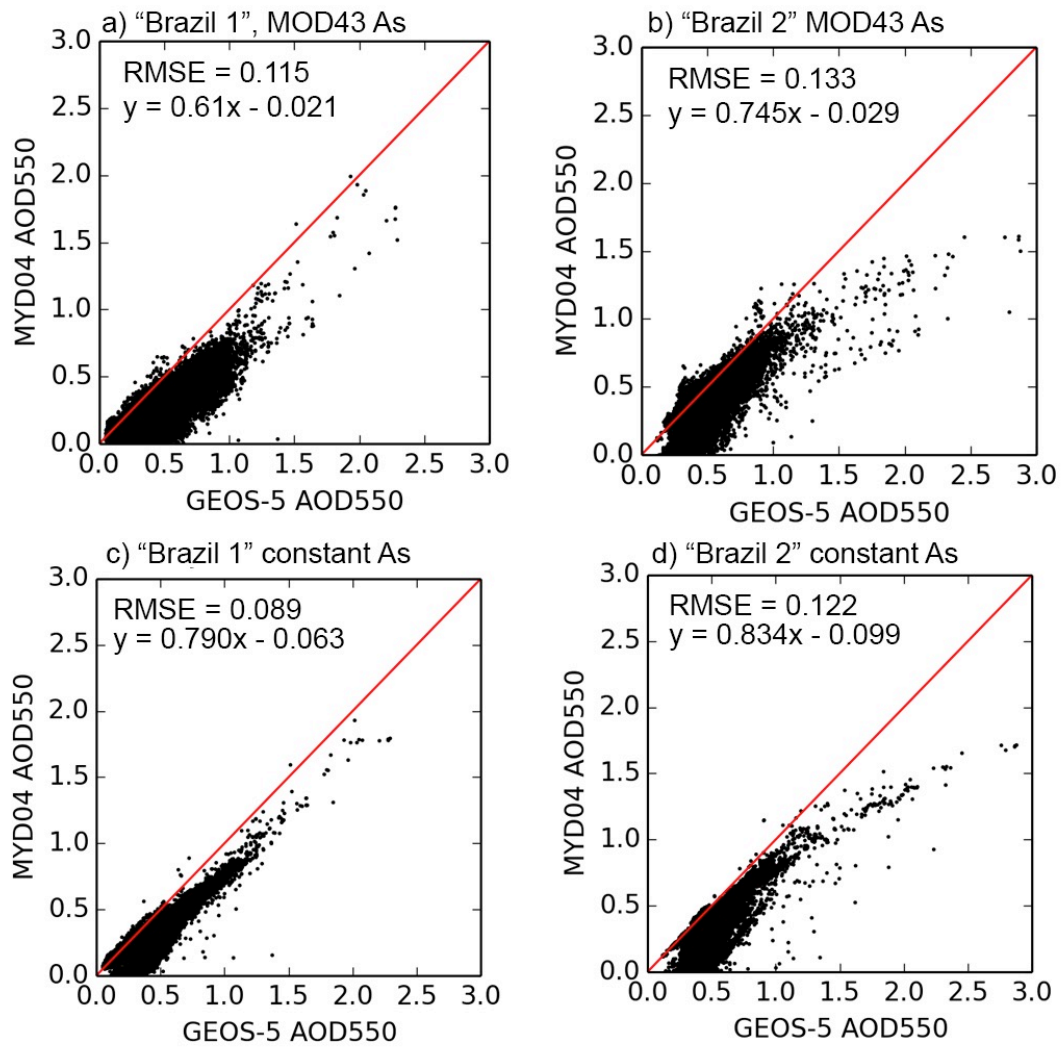
2   Figure 6. Surface albedo effect on Brazil smoke cases. Panels a) and c) show the runs with

3   MOD43-derived surface albedo. Panels b) and d) show the effect of selection of a constant

4   dark land surface albedo.
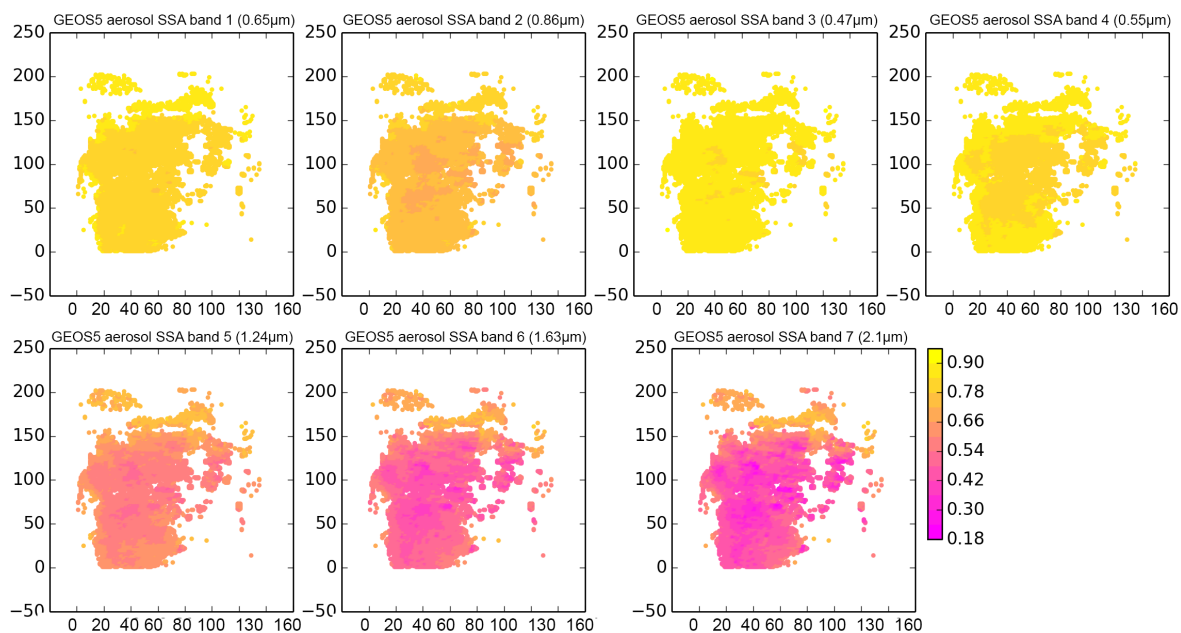
2   Figure 7. Bulk aerosol single scattering albedo for "Brazil 1" case for MODIS channels 1-7.

3   This single scattering albedo combines all aerosol species present in the scene.
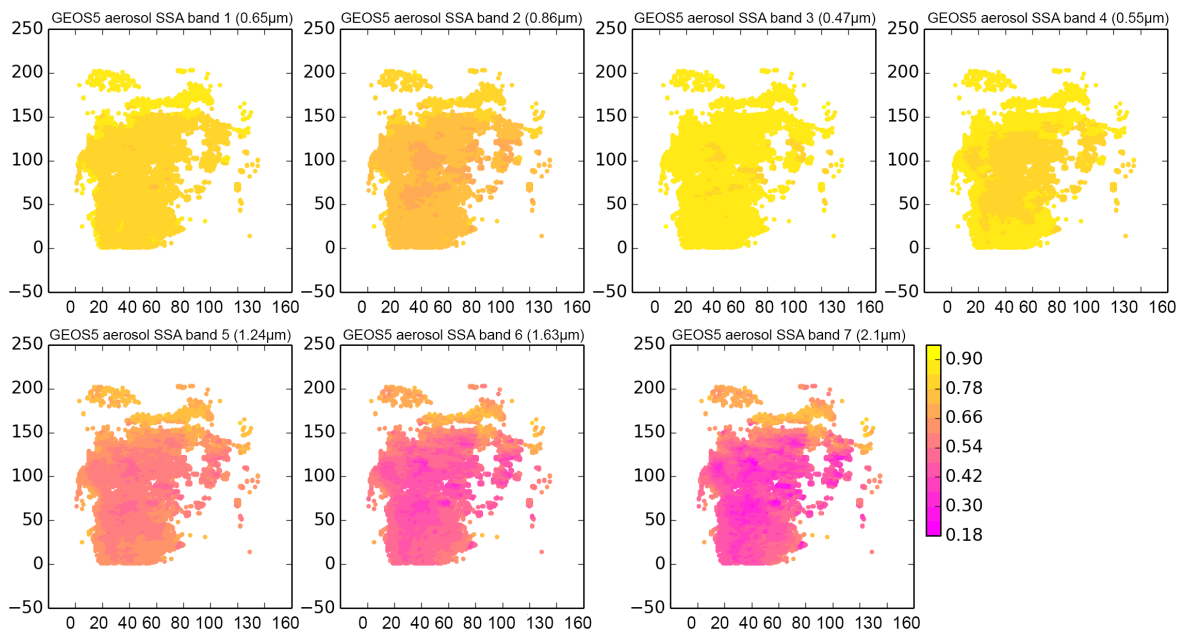
2   Figure 8. Bulk aerosol single scattering albedo for "Brazil 2" case for MODIS channels 1-7.

3   This single scattering albedo combines all aerosol species present in the scene.
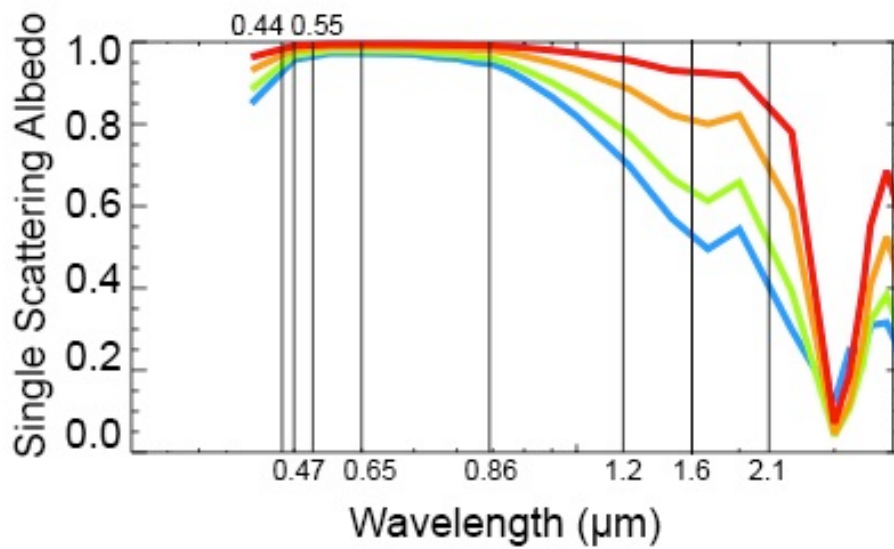
2   Figure 9. OPAC single scattering albedo as a function of humidity (color) and wavelength.

3   The various relative humidity levels are in order (red, orange, green and blue) for 95, 80, 30

4   and 0% column relative humidity.
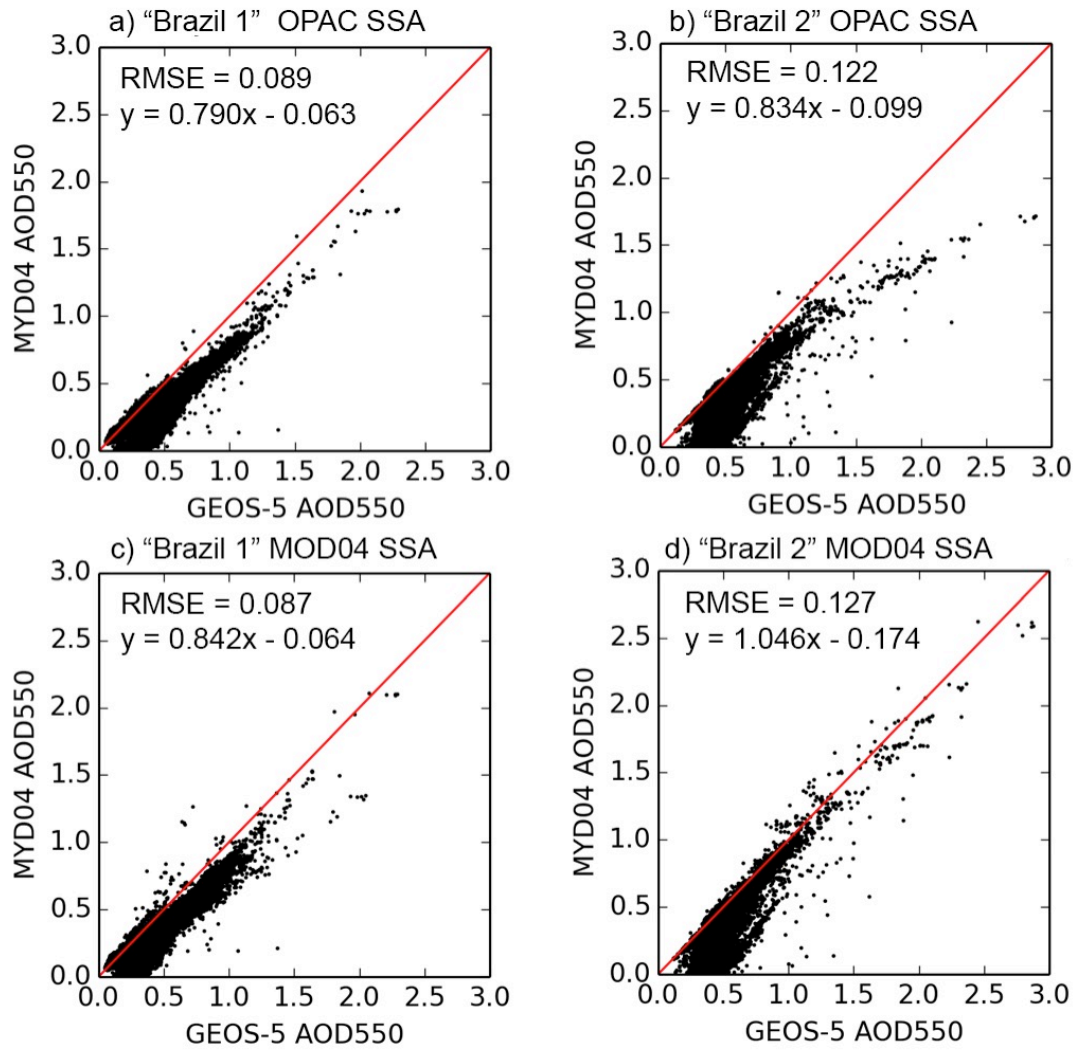
2 Figure 10. Impact of humidity on MOD04 retrieval illustrated via single scattering albedo

3 selection. Panels a) and c) show the "Brazil 1" case before and after the SSA adjustment.

4 Panels b) and d) show the same for "Brazil 2".
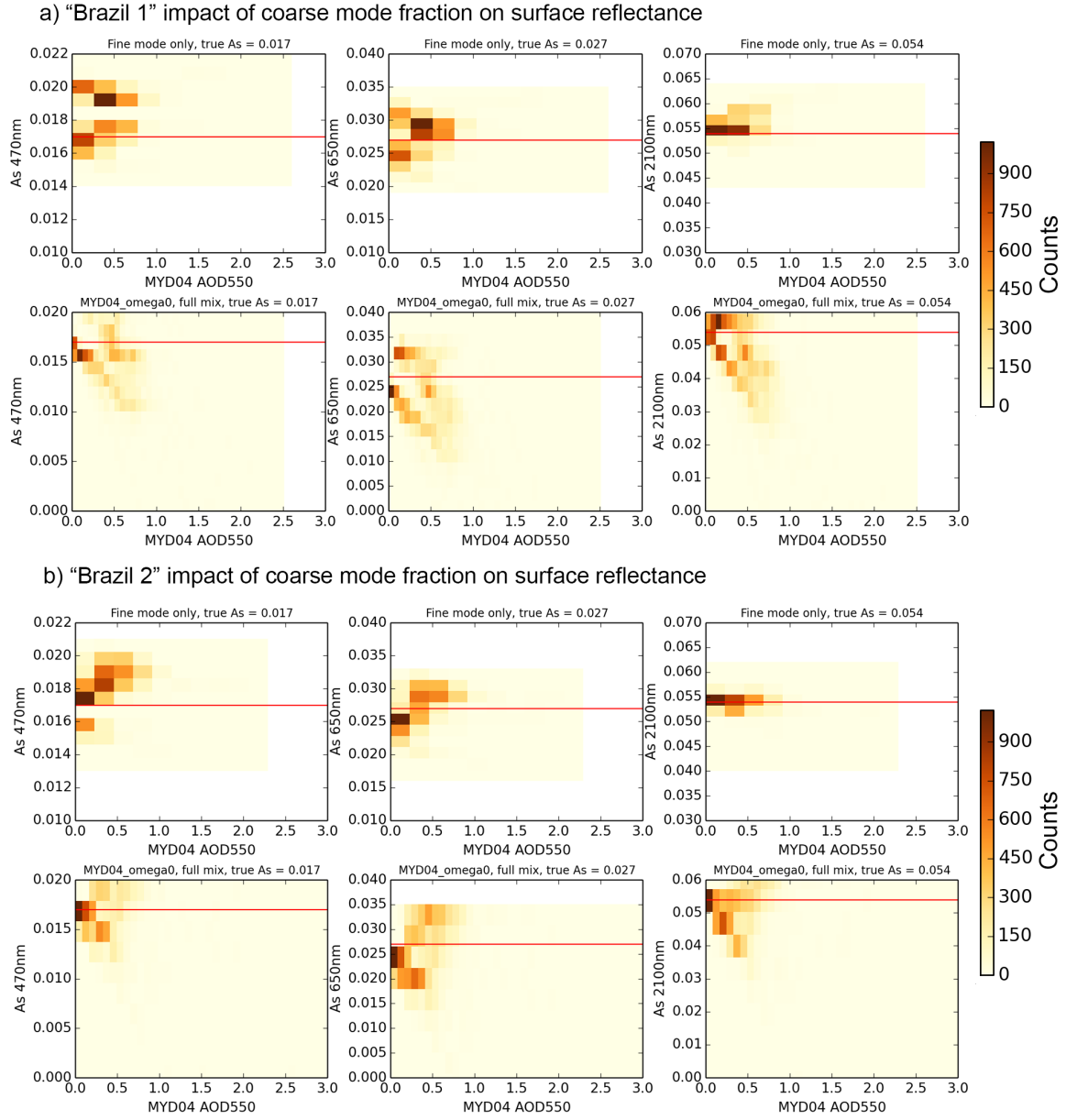
Figure 11. Impact of coarse mode fraction on MOD04 retrieved surface reflectance. Set a) shows the "Brazil 1" case and set b) shows "Brazil 2".